УДК 621.039.532.2 doi.org/10.31717/2311-8253.24.2.7

K. V. Simeiko[1, 2], O. P. Kozhan[2], M. A. Sydorenko[1], V. S. Ryabchuk[2], K. V. Lobach[3], O. M. Skoblyk[1], V. S. Havrylenko[1], P. A. Sabienin[1]

[1] *Institute for Safety Problems of Nuclear Power Plants of the NAS of Ukraine, 36a, Kirova st., Chornobyl, 07270, Ukraine*
[2] *Gas Institute of the NAS of Ukraine, 39, Dehtiarivska st., Kyiv, 03113, Ukraine*
[3] *National Science Center "Kharkiv Institute of Physics and Technology", 1, Akademichna st., Kharkiv, 61108, Ukraine*

Thermodynamic Calculations and Hydrodynamic Studies of the Process of High-Temperature Purification of Graphite in an Electrothermal Fluidized Bed

Ключові слова:
nuclear-purity graphite,
electrothermal fluidized bed,
hot filtration,
thermodynamics,
hydrodynamics

The general increase in electricity consumption and the development of nuclear energy, including next generation nuclear reactors where graphite-based materials are used, definitely leads to an increase in the need for its production. Therefore, the development and improvement of technologies for the production of high-purity graphite (including nuclear), namely the understanding of the thermodynamic and hydrodynamic processes of graphite purification, is of great practical importance. Thermodynamic calculations of the main chemical reactions of the high-temperature graphite purification process were carried out in the paper. For conducting thermodynamic calculations, a sample of natural graphite with a purity of up to 94.33% mass was taken. With the following composition of impurities: SiO_2–3.05 % mass; Al_2O_3–1.05% mass; Fe_2O_3–1.01% mass; CaO — 0.2% mass; MgO — 0.31% mass; S — 0.048% mass. The thermochemical parameters of the process were determined by the thermodynamic method ("TERRA" program). During the calculation, 0.9433 mol of C, 0.0305 mol of SiO_2, 0.0105 mol of Al_2O_3, 0.0101 mol of Fe_2O_3, 0.0002 mol of CaO, 0.0031 mol of MgO, 0.00048 mol of S, and 1 mol of N_2 were taken, temperature range is 300…3278 K, and pressure is 0.1 MPa. Obtained results show that at a temperature above 1600 K, part of the initial carbon is oxidized to CO, and nitrogen actually does not affect the process. And also taking into account that part of the substances CO; Si; SiC_2; SiS; Al; Fe; Mg; Ca; SiO at temperatures of 2800…3200 K are in a gas state and are carried to the purifier, from which we can conclude that the reaction temperature must be higher than 2800 K to carry out this process. The study of the hydrodynamic characteristics of graphite in a fluidized bed was carried out on the designed model installation with a fluidized bed. The working zone of the device is made in the form of a graphite cone with an opening angle of 25°, which provided the creation of a "spouted bed". Besides, part of the fluidizing agent (nitrogen) was supplied in a pulsating mode. For the research, 6 samples of graphite with different physical properties and chemical composition were chosen, the filling volume was 0.5 l. Based on thermodynamic calculations of the basic thermochemical reactions and cold hydrodynamic tests, a laboratory installation was created to monitor the process of high-temperature purification of graphite.

Introduction

Due to its unique properties, graphite has become an integral part of items used in nuclear power, power equipment, mechanical engineering, metallurgy and other industries. The field of application of graphite is constantly

© K. V. Simeiko, O. P. Kozhan, M. A. Sydorenko, V. S. Ryabchuk, K. V. Lobach, O. M. Skoblyk, V. S. Havrylenko, P. A. Sabienin, 2024. Ліцензія CC BY 4.0

expanding, thereby determining its consumer demand [1–7]. Taking this into account, graphite is already included in the list of strategic raw materials of the EU countries [1].

Other features of graphite as a material for nuclear physics include, first of all, a small effective cross-section σ of photonuclear reactions for carbon in the giant resonance region, associated with disruption of the natural oscillations of protons relative to neutrons (dipole oscillations) by γ-quanta. Nucleons can leave the nucleus not only during dipole oscillations, but also after their decay. A large part of collisions of neutrons with carbon nuclei occurs by the mechanism of elastic scattering, which led to the effective use of graphite as a neutron moderator or absorber [8].

Graphite is a good construction material, due to the very high temperature of sublimation, graphite remains solid (in an oxygen-free atmosphere) up to temperatures of the order of 4273 K. At the same time, at a low density, graphite is a material that is not only solid, but also easily processed mechanically, has a low pressure of saturated vapors in a vacuum even at elevated temperatures. Graphite has high thermal conductivity and heat capacity, at the same time not necessarily having high electrical conductivity. This material in the temperature range of its use increases its strength with increasing temperature, has corrosion and erosion resistance during irradiation [9]. The strength of graphite varies significantly depending on the method of its production, therefore graphites with the identical density, but differing in structure, can have different strengths. The general rule is that a more finely structured graphite composite has greater strength and longer service life, as a rule [10].

Graphite as a structural and functional material was used in high-temperature reactors: AVR (Germany), HTGR-1 (USA), improved reactor with gas cooling AGR (England), and in high power channel-type reactors (HPCR) (USSR, RF, Lithuania) [11]. Currently, graphite is a structural and functional material in nuclear power systems of the IV generation, in particular, in high-temperature gas cooled (HTGR, HTR, HTGR, VHTR) and molten salt reactors (MSR) [12].

With the development of nuclear power systems of the IV generation and the increase in the popularity of electric transport, there is a dynamic increase in the consumption of graphite [13–16], therefore the issue of developing and improving technologies for the production of high-purity graphite (including nuclear) is of great practical importance.

An overview of modern graphite purification technologies is described by the authors in [17].

Thermodynamic calculations of the main chemical reactions of the high-temperature graphite purification process

The research is based on the idea of high-temperature purification of graphite to high degrees of purity in an oxygen-free atmosphere without the use of harmful halogen-containing compounds.

The task of the research as a whole is to determine the fundamental possibility of purifying natural graphite to nuclear purity by means of its high-temperature treatment in an electrothermal fluidized bed (ETFB).

For research, 6 samples of natural graphite were taken, the characteristics of which are presented in Table. 1.

The use of a fluidized bed (FB) should allow heat to be evenly distributed between graphite particles, and the formation of a microdischarge plasma will allow reaching the required temperatures.

Thermodynamic methods ("TERRA" program) were used to determine the thermochemical parameters of the process.

Natural graphite with a purity of up to 94.33 % mass was chosen for the study with the following composition of impurities: SiO_2 — 3.05 % mass; Al_2O_3 — 1.05 % mass; Fe_2O_3 — 1.01 % mass; CaO — 0.2 % mass; MgO — 0.31 % mass; S — 0.048 % mass. During the calculation, 0.9433 mol of C, 0.0305 mol of SiO_2, 0.0105 mol of Al_2O_3, 0.0101 mol of Fe_2O_3, 0.0002 mol of CaO, 0.0031 mol of MgO, 0.0031 mol of MgO, 00048 mol of S and 1 mol N_2 were taken, temperature range is 300…3278 K, pressure is 0.1 MPa:

The equilibrium curves of the system are shown in Fig. 1.

For a more convenient perception of impurity concentrations, let's make a graph excluding carbon, nitrogen and CO (Fig. 2).

The equilibrium composition of the system is given in Tables 2–4.

From these calculations, it can be seen that above 1600 K, part of the initial carbon is oxidized to CO. Nitrogen actually does not affect the processes.

The main thermophysical characteristics of this process are given in Table 5, where T is temperature, K, S_{ENTR} is entropy, kJ/kg K, I_{ENTL} is total enthalpy, U_{IE} is total internal energy, kJ/kg, MMg is the molar mass of the gas phase, Cp' is the specific heat capacity, $Cp'g$ is heat capacity of gas phase, kJ/(kg · K).

Considering that part of the CO; Si; SiC_2; SiS; Al; Fe; Mg; Ca; SiO substances at temperatures of 2800…3200 K are in a gaseous state and carried to the purifier, the meth-

Table 1. Characteristics of natural graphite samples

Parameter	Sample					
	No. 1	No. 2	No. 3	No. 4	No. 5	No. 6
Content of chemical components, % mass:						
Ph	9.2	9.2	8.6	9.4	8.1	9.0
C	91.0	90.4	92.4	92.3	93.1	93.0
Al	8.8	9.4	7.3	7.6	6.8	6.8
W	0.2	0.2	0.5	0.3	0.2	0.17
V	0.2	0.2	0.3	0.1	0.1	0.2
Bulk density, g/l	482	430	553	377	466	651
Tap density, g/l	610	580	710	500	600	570
Granulometric composition, %:						
500 μm	–	–	–	–	–	–
400 μm	–	–	–	–	–	–
315 μm	–	–	0.1	–	–	–
200 μm	0.4	0.1	7.2	0.2	0.3	–
180 μm	1.0	0.6	5.5	0.3	1.0	0.1
160 μm	4.4	1.1	6.5	0.7	3.1	1.1
150 μm	4.8	2.3	5.9	1.1	4.9	2.2
100 μm	36.1	20.6	25.6	10.2	33.3	23.6
71 μm	23.5	23.9	19.3	23.8	25.3	31.5
63 μm	7.9	9.1	10.3	14.8	10.7	12.3
45 μm	9.9	18.3	9.3	19.3	10.7	14.6
–45 μm	12.0	24.0	10.3	29.6	10.7	14.6

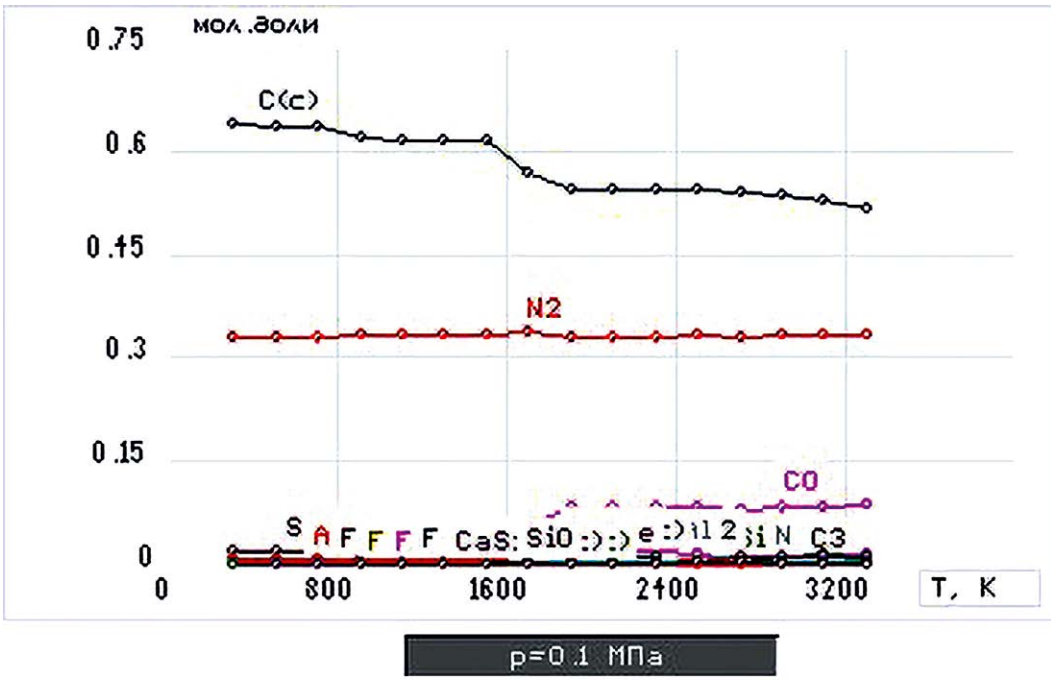

Fig. 1. Equilibrium curves of the system "C + SiO_2 + Al_2O_3 + Fe_2O_3 + CaO + MgO + S + N_2 0.9433 : 0.0305 : 0.0105 : 0.0101 : 0.0002 : 0.0031 : 0.00048 : 1"

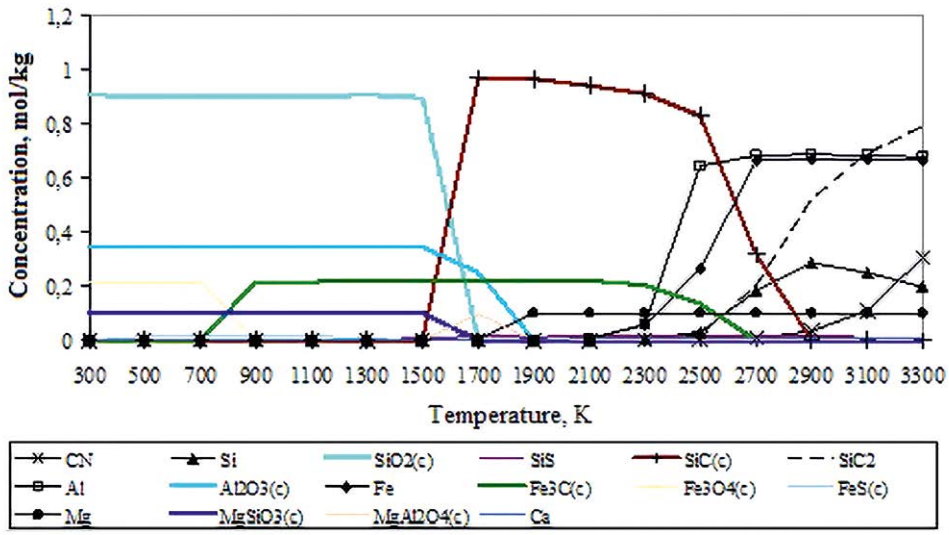

Fig. 2. Equilibrium curves of the system "C + SiO_2 + Al_2O_3 + Fe_2O_3 + CaO + MgO + S+ N_2 0.9433 : 0.0305 : 0.0105 : 0.0101 : 0.0002 : 0.0031 : 0.00048 : 1" (excluding carbon, nitrogen and CO)

od of high-temperature purification of graphite to high degrees of purity must be effective.

Determination of hydrodynamic features of fluidization of natural graphite on a cold model

Natural graphite powder, due to the platelet (lamellar) shape of its particles, is an inconvenient material for creating a FB. During blowing it with gas, instead of the usual bubble boiling, one or more channels are formed, through which most of the gas passes. In order to pass the bubble boiling of the material and ensure the possibility of continuous operation of the installation (loading/unloading without cooling of the installation), the working zone of the reactor is made in the form of a graphite cone with an opening angle of 25°, which ensured the creation of a "spouted bed". In addition, part of the fluidizing agent (nitrogen) was supplied in a pulsating mode.

The experiments were carried out in the cold mode of operation of the ETFB laboratory installation with the outer cover open to determine the optimal parameters for supplying the fluidizing agent (nitrogen) to the working area, which would ensure good mixing of the material in the working area. At the first stage, nitrogen was supplied in a single flow in a stationary and pulsating mode in the center of the working area. Graphite samples Nor. 1–7 with a filling volume of 0.5 l were selected for the research. The schematic picture of material fluidization is presented in Fig. 3.

Based on the results of visual observation of the fluidization nature, it can be noted that the boiling of sample No. 6 was characterized by the formation of a channel and the ejection of material at the point that was above the hole for nitrogen supply and the finished material discharge. The boiling of sample No. 5 was similar to that of sample No. 6, but it was characterized by a smaller emission of graphite particles. During the boiling of sample No. 4, the working area was heavily "dusted" with finely dispersed material, which prevented the visual control of the process. Higher values of the nitrogen flow did not ensure proper boiling and mixing of the material, but only caused a higher discharge of the material through the channel and an increase in the removal of the material. Lower values of nitrogen consumption led to the "laying down" of graphite material. The material of samples No. 2 and No. 3 was generally in a stationary state and only under mechanical influence, a channel was formed in it through which nitrogen passed. Practically the same picture also occurred for sample No. 1.

To assess the possibility of intensification of fluidization of the material, similar experiments were conducted on a cold model of the working zone of the laboratory installation with an additional supply of nitrogen through side holes in the peripheral electrode. The visual picture of fluidization is shown in Fig. 4.

Additional supply of nitrogen through side channels increased the intensity and degree of homogeneity of boiling, however, during pulsations and when the supply was stopped, the material flowed through these holes into the cold zone of the reactor (outside the peripheral electrode). Therefore, in order to avoid the removal of graphite material during experiments on heat treatment of graphite, it was

Table 2. The equilibrium composition of the system "C + SiO_2 + Al_2O_3 + Fe_2O_3 + CaO + MgO + S + N_2 0.9433 : 0.0305 : 0.0105 : 0.0101 : 0.0002 : 0.0031 : 0.00048 : 1" (mol /kg)

T	N_2	C(c)	CO	CN	Si	SiO_2
300	16.5158	31.8558	3.59E-11	1.93E-22	1.93E-22	0.904849
500	16.5158	31.8505	4.24E-05	1.93E-22	1.93E-22	0.898249
700	16.5158	31.8428	0.015449	1.93E-22	1.93E-22	0.898249
900	16.5158	30.8556	0.690432	1E-19	1.93E-22	0.898249
1100	16.5158	30.7066	0.988257	4.38E-15	1.93E-22	0.898249
1300	16.5158	30.6927	1.00374	7.01E-12	2.11E-16	0.904845
1500	16.5158	30.6717	1.02286	1.55E-09	1.95E-10	0.895677
1700	16.5158	27.7346	2.98863	1E-07	2.27E-07	1E-30
1900	16.1687	26.6007	4.12938	2.59E-06	0.000011	1E-30
2100	16.17	26.6468	4.11041	3.56E-05	0.000245	1E-30
2300	16.202	26.7137	4.08349	0.000309	0.003171	1E-30
2500	16.5125	26.8634	4.03821	0.001956	0.028484	1E-30
2700	16.5034	27.0783	4.02613	0.009271	0.182607	1E-30
2900	16.4794	26.6359	4.10524	0.035102	0.287433	1E-30
3100	16.4178	26.0983	4.14568	0.111012	0.249027	1.15E-27
3300	16.2695	25.1775	4.15654	0.304904	0.195782	2.86E-30

Table 3. The equilibrium composition of the system "C + SiO_2 + Al_2O_3 + Fe_2O_3 + CaO + MgO + S + N_2 0.9433: 0.0305: 0.0105: 0.0101: 0.0002: 0.0031: 0.00048: 1" (mol /kg)

T	SiS	SiC(c)	SiC_2	Al	Al_2O_3	Fe	Fe_3C
300	1.93E-22	1E-30	1.93E-22	1.93E-22	0.347129	1.93E-22	1E-30
500	1.93E-22	1E-30	1.93E-22	1.93E-22	0.347129	1.93E-22	1E-30
700	1.93E-22	1E-30	1.93E-22	1.93E-22	0.347129	1.93E-22	1E-30
900	1.18E-21	1E-30	1.93E-22	1.93E-22	0.347129	9.1E-16	0.21656
1100	1.3E-12	1E-30	1.93E-22	1.93E-22	0.347129	1.46E-11	0.21661
1300	3.21E-06	1E-30	6.96E-20	7.4E-16	0.347129	1.14E-08	0.219052
1500	0.00875	1E-30	5.43E-13	1.32E-10	0.347129	1.47E-06	0.221844
1700	0.015843	0.97136	3.19E-09	3.45E-07	0.248792	5.59E-05	0.221825
1900	0.010174	0.964793	5.47E-07	5.79E-05	1.68E-28	0.000931	0.221534
2100	0.015825	0.940029	3.33E-05	0.002617	1E-30	0.008648	0.218961
2300	0.015797	0.91188	0.000986	0.060511	1E-30	0.054233	0.203766
2500	0.015749	0.829023	0.017608	0.644204	1E-30	0.264013	0.133839
2700	0.015708	0.314833	0.201436	0.684619	1E-30	0.665531	1.37E-26
2900	0.015198	5.54E-26	0.519755	0.687619	1E-30	0.665528	1E-30
3100	0.012531	1.15E-27	0.690585	0.684705	1.15E-27	0.665519	1.15E-27
3300	0.006462	2.86E-30	0.787044	0.677185	2.86E-30	0.665494	2.86E-30

Table 4. The equilibrium composition of the system "C + SiO_2 + Al_2O_3 + Fe_2O_3 + CaO + MgO + S + N_2 0.9433 : 0.0305 : 0.0105 : 0.0101 : 0.0002 : 0.0031 : 0.00048 : 1" (mol /kg)

T	Fe_3O_4	FeS	Mg	$MgSiO_3$	$MgAl_2O_4$	Ca
300	0.219198	8.73E-26	1.93E-22	0.101673	1E-30	1.93E-22
500	0.216553	0.015874	1.93E-22	0.101673	1E-30	1.93E-22
700	0.216553	0.015874	1.93E-22	0.101673	1E-30	1.93E-22
900	1E-30	0.015853	6.68E-21	0.101673	1E-30	1.93E-22
1100	1E-30	0.015701	5.45E-14	0.101673	1E-30	4.06E-20
1300	1E-30	0.008377	3.94E-09	0.101673	1E-30	1.07E-14
1500	1E-30	9.11E-29	1.37E-05	0.101659	1E-30	1.32E-10
1700	1E-30	1E-30	0.003334	2.42E-28	0.098337	7.44E-07
1900	1E-30	1E-30	0.101663	1E-30	4.15E-29	0.000926
2100	1E-30	1E-30	0.101668	1E-30	1E-30	0.006599
2300	1E-30	1E-30	0.101671	1E-30	1E-30	0.006597
2500	1E-30	1E-30	0.101672	1E-30	1E-30	0.006596
2700	1E-30	1E-30	0.101672	1E-30	1E-30	0.006586
2900	1E-30	1E-30	0.101671	1E-30	1E-30	0.006561
3100	1.15E-27	1.15E-27	0.101666	1.15E-27	1.15E-27	0.006507
3300	2.86E-30	2.86E-30	0.101656	2.86E-30	2.86E-30	0.006399

Table 5. Thermophysical characteristics of the graphite purification process in the system "C + SiO_2 + Al_2O_3 + Fe_2O_3 + CaO + MgO + S+ N_2 0.9433 : 0.0305 : 0.0105 : 0.0101 : 0.0002 : 0.0031 : 0.00048 : 1"

T	S_{ENTR}	I_{ENTL}	U_{IE}	Cp'	MMg	Cp'g
300	3.463	–1836.07	–1836.33	0.868105	28.0657	1.03964
500	3.96746	–1636.52	–1664.35	1.09949	28.0771	1.05506
700	4.36624	–1398.47	–1453.89	1.28715	28.0696	1.10121
900	4.85966	–1004.42	–1091.29	1.7041	28.1551	1.14742
1100	5.16411	–701.943	–818.675	1.43207	28.0181	1.18605
1300	5.40897	–408.561	–554.503	1.46715	28.015	1.21837
1500	5.63026	–98.667	–274.018	0	28.0304	1.24355
1700	6.19055	800.53	572.822	1.55988	28.049	1.26386
1900	6.52949	1402.58	1130.3	1.53444	28.037	1.27762
2100	6.68637	1716.1	1409.48	1.59609	28.0749	1.28859
2300	6.85231	2081.93	1738.94	2.32702	28.161	1.31578
2500	7.18254	2877.86	2479.37	2.79016	28.4868	1.45347
2700	7.4615	3604.48	3152.71	4.54308	29.269	1.50295
2900	7.67097	4187	3688.32	2.18372	29.5018	1.53879
3100	7.81788	4627.68	4087.09	2.3405	29.5847	1.61597
3300	7.99715	5202.58	4616.29	3.74655	29.6971	1.85524

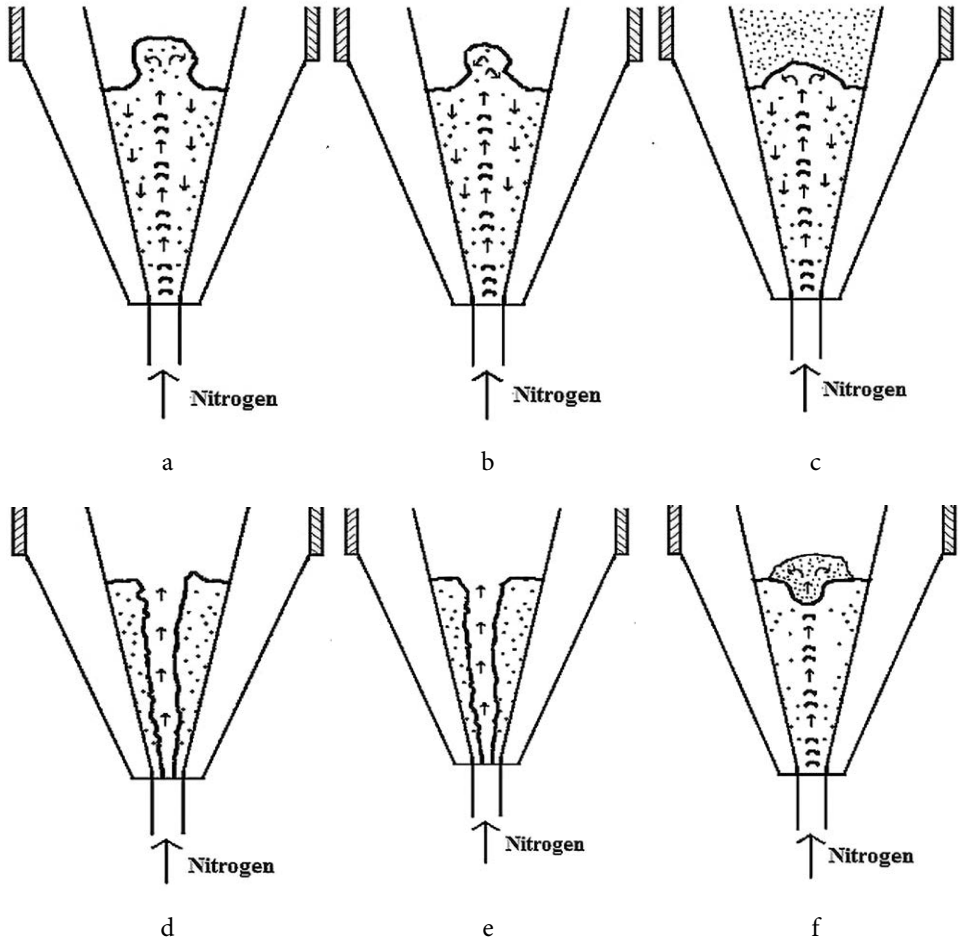

Fig. 3. Character of natural graphite particles fluidization in the "cold" mode of operation of the ETFB installation: a — No. 6, b — No. 5, c — No. 4, d — No. 3, e — No. 2, f — No. 1

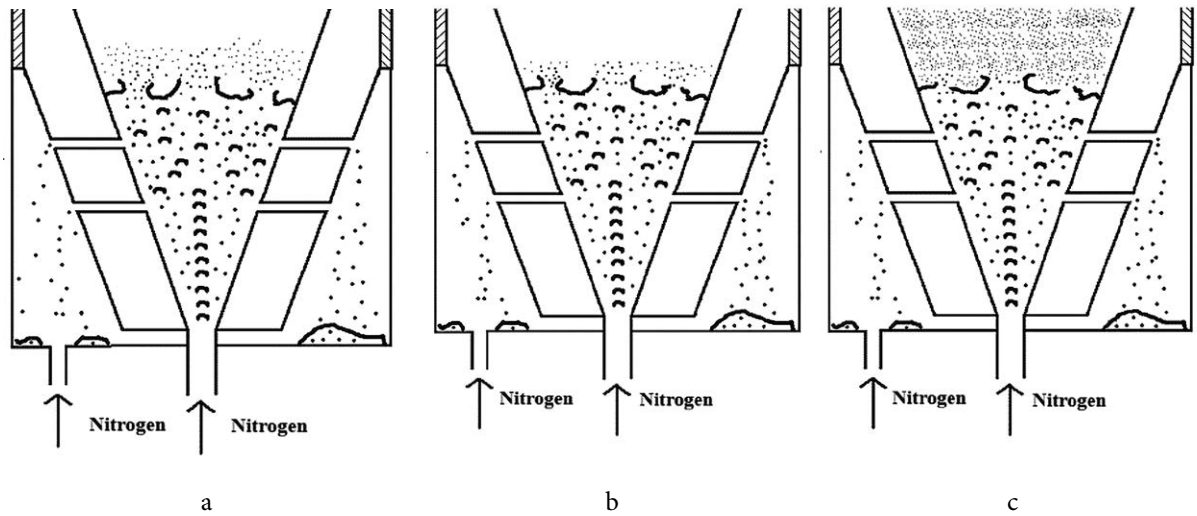

Fig. 4. The nature of natural graphite particles fluidization in a cold model of the working area of a laboratory installation with ETFB with additional holes for nitrogen supply: a — sample No. 5, b — sample No. 6, c — sample No. 4

decided to temporarily abandon the additional holes in the peripheral electrode of the ETFB laboratory installation.

Laboratory installation for researching the process of the natural graphite high-temperature purification

The laboratory installation with ETFB is designed to determine the principle possibility of enriching natural powdered graphite to a carbon content of 99.9% mass. using its high-temperature (over 2273 K) treatment in an inert atmosphere. The choice of a gas distribution device in the form of a cone is due to the creation of conditions for the continuity of the process (unloading/loading the reaction zone of the reactor without cooling the installation). The scheme of the reactor is presented in Fig. 5.

The reactor works as follows: through the fittings 1 and 2, through the pipe 3, nitrogen is supplied to the reaction zone 4 in stationary and pulsating mode, respectively. Nitrogen exits into the atmosphere through pipe 5 and cyclone cleaner 6. Through the hole for monitoring the process 7, the starting material is loaded into the reaction zone 4 and a current is supplied to the electrode 8. The lower 9 and upper 10 covers are cooled with water. The height of the electrode is regulated by a worm-type mechanism 11. The temperature is measured by a pyrometer through the hole 12 and a thermocouple 13. After the process, the material is unloaded into the bunker 14. The outer layer of thermal insulation 15 is made of heat-resistant wool MKRR-130, the inner layer 16 is made of technical carbon. The outer cylindrical case is made of stainless steel X18H10T.

The basic technological scheme is shown in Fig. 6.

The appearance of the installation is shown in Fig. 7.

The installation works as follows: cooling water is supplied to the reactor 1 by opening the ball valve 2, nitrogen is supplied to the gas distribution comb 4 by opening the shut-off valve on the cylinder 3, then nitrogen is supplied in stationary mode by opening the valve 5 through the rotameter 6. By opening the valve 7 through the rotameter 8, the receiver 9 and the pulsator 10 supply nitrogen in a pulsating mode. Nitrogen, after passing through reactor 1, enters the purifier 11 and the hood 12. Material is loaded through the observation window 13. By turning on the switch 14, current is supplied to the reactor 1 through the transformer 15 and the electrode 16.

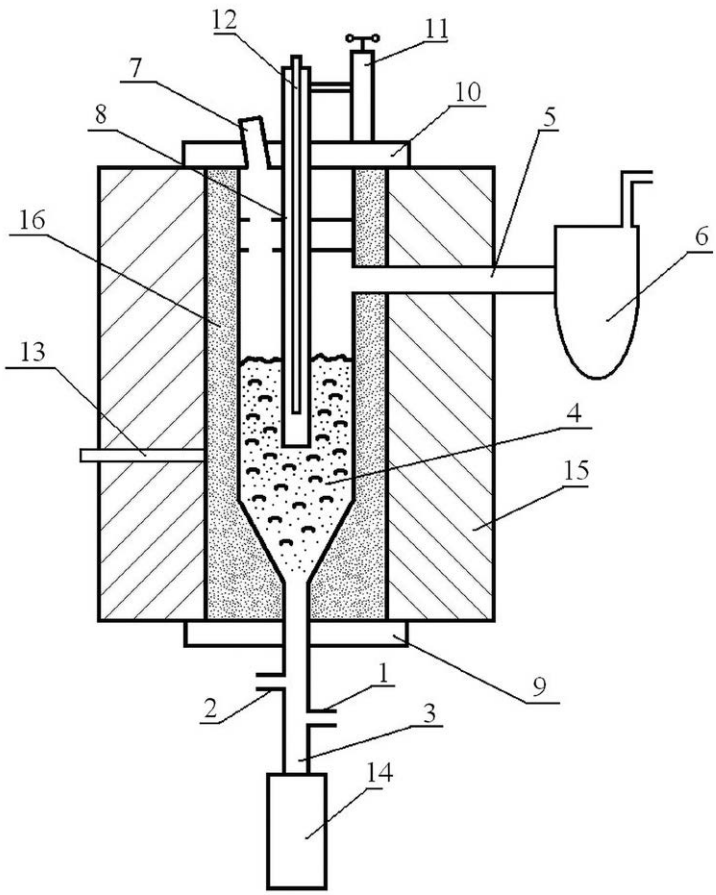

Fig. 5. Scheme of the reactor of the laboratory installation for researching the process of natural graphite purification:
1 — fitting for nitrogen supply in stationary mode,
2 — fitting for nitrogen supply in pulsating mode,
3 — pipe for nitrogen supply, 4 — reaction zone (FB),
5 — pipe for nitrogen removal, 6 — cyclone cleaner,
7 — hole for tracking the process/material loading,
8 — electrode, 9 — lower water cooling cover,
10 — upper water cooling cover, 11 — mechanism for adjusting the height of the electrode, 12 — hole for tracking radiation for the pyrometer,
13 — thermocouple, 14 — bunker for cooling the finished product, 15 — external thermal insulation,
16 — internal thermal insulation

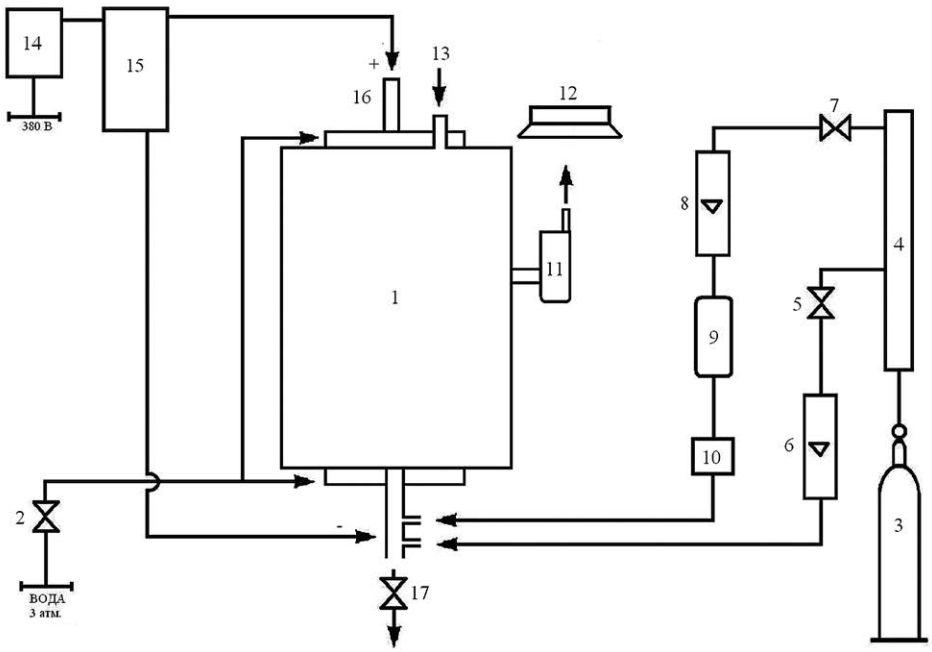

Fig. 6. Basic technological diagram of a laboratory installation for cleaning natural graphite:
1 — reactor with ETFB, 2 — ball valve, 4 — gas distribution comb, 5, 7 — valves, 6, 8 — rotameter,
9 — receiver, 10 — pulsator, 11 — cyclone cleaner, 12 — hood, 13 — window for observation/loading material,
14 — switch, 15 — power transformer, 16 — electrode, 17 — unloading and cooling system

Fig. 7. The appearance of the laboratory installation
for the research of the natural graphite purification process

Table 6. The value of the operating parameters of the laboratory installation for the research of the process of natural graphite high-temperature purification

Parameter	Unit of measurement	A measurement value or range
The volume of the reaction zone	m^3	0.0015
Type of gas distribution device		cone
The type of electric current between the electrodes		Removable
Amperage	A	0…400
High-voltage	B	20…60
Material processing temperature	°C	1500…3000
Duration of material processing	h	0.5…1.5

After the process, the material is unloaded through the unloading and cooling system 17.

Table 6 shows the ranges of changes in the operating parameters of the laboratory installation for the research of high-temperature purification of natural graphite.

Pyrometers Promyn (Ukraine) and FLUS IR-866 U (China) will be used to measure the temperature.

Basic principles of experimental research

The results of preliminary thermodynamic calculations show that some of the impurities pass into the gas phase according to their evaporation temperature. Another part of the impurities, namely among themselves, forms compounds that also pass into the gas phase (for example, Fe_3C at temperatures above 1923 decomposes into Fe and carbon) and are carried to the purifier with inert gas. The calculated range of temperatures at which graphite reaches a high degree of purity is 2573…2873 K. Part of the graphite can interact with oxygen, which is formed from oxide impurities and be carried into the purifier in the form of CO. Estimated losses of graphite from oxidation to CO will be 7…10% mass.

Conclusions

1. Part of the substances (Si; SiC_2; SiS; Al; Fe; Mg; Ca; SiO) that should be formed during the process of high-temperature purification of graphite at temperatures above 2800 K are in a gaseous state. Therefore, to carry out this process, the reaction temperature must be above 2800 K.

2. On the basis of thermodynamic calculations of the main thermochemical reactions, a laboratory installation for researching the process of high-temperature graphite purification was developed and cold hydrodynamic tests were created.

References

1. Toniolo B. (2016). *European Carbon and Graphite Association ECGA. Annual Report 2014–2015.* Bruxelles, Belgium: EGGA, 19 p. Available at: http://www.ecga.net/sites/default/files/pdf/ecga_ar_2014–15_draft-final.pdf.
2. Jewell S., Kimball S. M. (2017). *Mineral commodity summaries 2017.* U. S. Geological Survey, Reston, U.S., 202 p., doi.org/10.3133/70180197.
3. Olson D. W. (2014). *Graphite. U. S. Geological Survey Minerals Yearbook — 2014 Graphite [Advance release].* U. S. Department of the Interior, U. S. Geological Survey, 15 p.
4. Keeling J. (2017). Graphite: properties, uses and South Australian resources. *MESA Journal*, vol. 84 (3), pp. 28–41.
5. Siow K. S. (2017). Graphite Exfoliation to Commercialize Graphene Technology. *Sains Malaysiana*, vol. 46 (7), pp. 1047–1059. doi.org/10.17576/jsm-2017–4607–06.
6. Kalyoncu R. S. (2000). *Graphite. U. S. Geological Survey Minerals Yearbook*. Reston, US: U. S. Geological Survey, pp. 76–77.
7. Crossley P. (2000). Graphite: high-tech supply sharpens up. *Industrial Minerals*, vol. 398, pp. 31–47.
8. Vasilenko I. Ya., Osipov V. A., Rublevskij V. P. (1992). *Radioaktivnyj uglerod* [Radioactive carbon]. *Priroda,* no. 12, pp. 59–65. (in Rus.)
9. Vlasova K. P. (1964). *Grafit kak vysokotemperaturnyj material* [Graphite as a high temperature material.]. Collection of articles. Moscow: Mir, 420 p. (in Rus.)
10. Zhmurikov Ye. I., Bubnenkov I. A., Dremov V. V., Samarin S. I., Pokrovskiy A. S., Kharkov D. V. (2013). *Grafit v nauke i yadernoj tekhnike* [Graphite in science and nuclear engineering]. Novosibirsk, 193 p. (in Rus.)
11. Dollezhal N. A., Yemelyanov I. Ya. (1980). *Kanalnyj yadernyj energeticheskij reaktor* [Channel nuclear power reactor], Moscow: Atomizdat, 208 p. (in Rus.)
12. Komir A. I., Odeychuk N. P., Nikolaenko A. A., Tkachenko V. I., Derevyanko V. A., Krivchenko O. V., She-

pelev A. G. (2016). [Graphite as a Structural Material for Generation IV Nuclear Energy Systems]. *Voprosy Atomnoj Nauki i Tehniki* [Issues of Atomic Science and Technology], vol. 1 (101), pp. 51–55. (in Rus.)
13. Barsukov V. Z., Khomenko V. G., Senik I. V., Chernyy O. Sh. (2013). [Lithium batteries for transport applications: modern problems and prospects]. *Voprosy Khimii i Khimicheskoj Tehnologii* [Issues of Chemistry and Chemical technology], no. 4, pp. 127–131. (in Rus.)
14. Moradi B., Botte G. G. (2016). Recycling of graphite anodes for the next generation of lithium ion batteries. *Journal of Applied Electrochemistry*, vol. 46 (2), pp. 123–148. doi.org/10.1007/s10800-015-0914-0.
15. Li J., Henry F., Feng Y. (2017). How to develop best carbon/graphite products for lead-carbon battery applications (Superior Graphite). Poster session presented at the *10th International conference on lead-acid batteries LABAT'2017, (Golden Sands, Bulgaria 13–16 June 2017)*, p. 23.
16. Elementenergy. *Cost and performance of EV batteries* (Final report for The Committee on Climate Change). Retrieved from Elementenergy, 2012, 91 p.
17. Simeiko K. V., Kupriianchuk S. V., Syniahovskyi A. O. (2023). Technologies and Promising Developments of Graphite Production (Overview). *Nuclear Power and the Environment*, vol. 4 (26), pp. 9–23. doi.org/10.31717/2311-8253.23.1.2. (in Ukr.)

Сімейко К. В.[1,2], Кожан О. П.[2], Сидоренко М. А.[1], Рябчук В. С.[2], Лобач К. В.[3], Скоблик О. М.[1], Гавриленко В. С.[1], Сабєнін П. А.[1]

[1]Інститут проблем безпеки АЕС НАН України, вул. Кірова, 36а, Чорнобиль, 07270, Україна
[2]Інститут газу НАН України, вул. Дегтярівська, 39, Київ, 03113, Україна
[3]Національний науковий центр "Харківський фізико-технічний інститут", вул. Академічна, 1, Харків, 61108, Україна

Термодинамічні розрахунки та гідродинамічні дослідження процесу високотемпературного очищення графіту в електротермічному псевдозрідженому шарі

Загальне збільшення споживання електроенергії та розвиток ядерної енергетики, в тому числі ядерних реакторів нового покоління, де застосовуються матеріали на основі графіту, безумовно веде до зростання необхідності його виготовлення. Тому розробки та вдосконалення технологій виробництва графіту високої чистоти (у тому числі ядерної), а саме розуміння термодинамічних та гідродинамічних процесів очищення графіту, мають велике практичне значення.

У роботі проведено термодинамічні розрахунки основних хімічних реакцій процесу високотемпературного очищення графіту. Для проведення термодинамічних розрахунків був взятий зразок природного графіту з чистотою до 94,33 %мас. зі складом домішок: SiO_2 — 3,05 %мас.; Al_2O_3 — 1,05 %мас.; Fe_2O_3 — 1,01 %мас.; CaO — 0,2 %мас.; MgO — 0,31 %мас.; S — 0,048 %мас. Термохімічні параметри процесу визначалися термодинамічним методом (програма TERRA). Під час проведення розрахунку було взято 0,9433 моль C, 0,0305 моль SiO_2, 0,0105 моль Al_2O_3, 0,0101 моль Fe_2O_3, 0,0002 моль CaO, 0,0031 моль MgO, 0,00048 моль S та 1 моль N_2, діапазон температур: 300…3278 К, тиск 0,1 МПа. З отриманих результатів видно, що за температури вище 1600 К частина вихідного вуглецю окислюється до CO, а азот фактично не впливає на проходження процесів. А також враховуючи, що частина речовин CO; Si; SiC_2; SiS; Al; Fe; Mg; Ca; SiO за температур 2800…3200 К перебувають у газовому стані та виносяться в очисник, з чого можна зробити висновок, що для проведення цього процесу температура реакції має бути вище 2800 К.

Вивчення гідродинамічних особливостей графіту у псевдозрідженому шарі проводилось на створеній модельній установці з псевдозрідженим шаром. Робоча зона апарату виконана у вигляді графітового конуса з кутом розкриття 25°, що забезпечувало створення «фонтануючого шару». Крім того, частина зріджуючого агенту (азоту) подавалася в пульсуючому режимі. Для проведення досліджень було обрано 6 зразків графіту з різними фізичними властивостями і хімічним складом, об'єм засипки 0,5 л.

На основі термодинамічних розрахунків основних термохімічних реакцій розроблено та холодних гідродинамічних випробувань створено лабораторну установку для дослідження процесу високотемпературного очищення графіту.

Ключові слові: графіт ядерної чистоти, електротермічний псевдозріджений шар, високотемпературна очистка, термодинаміка, гідродинаміка.

Надійшла 08.08.2024
Received 08.08.2024